Chinese Chemical Letters 35 (2024) 109078

Contents lists available at ScienceDirect

Chinese Chemical Letters

journal homepage: www.elsevier.com/locate/cclet

MXene–derived quantum dots based photocatalysts: Synthesis, application, prospects, and challenges

Hao Deng[a], Yuxin Hui[a], Chao Zhang[a], Qi Zhou[a], Qiang Li[a,*], Hao Du[a], Derek Hao[c], Guoxiang Yang[a,b], Qi Wang[a,b,*]

[a] School of Environmental Science and Engineering, Zhejiang Gongshang University, Hangzhou 310018, China
[b] Instrumental Analysis Center of Zhejiang Gongshang University, Hangzhou 310018, China
[c] Centre for Technology in Water and Wastewater (CTWW), School of Civil and Environmental Engineering, University of Technology Sydney (UTS), Ultimo, NSW 2007, Australia

ARTICLE INFO

Article history:
Received 4 May 2023
Revised 7 August 2023
Accepted 8 September 2023
Available online 9 September 2023

Keywords:
MXenes
Quantum dots
Photocatalysis
Composites
Environment purification

ABSTRACT

In recent years, the emerging two–dimensional material–MXenes has attracted widespread attention in the field of photocatalysis due to its high conductivity, suitable Fermi level, tunable elemental composition, and excellent photoelectric properties. The zero–dimensional quantum dots (MQDs) derived from 2D MXenes not only inherit the characteristics of MXenes but also exhibit better performance due to the quantum size effect. Based on the above excellent physical and chemical properties, MQDs are often used as co–catalysts of photocatalysts, and show excellent co–catalytic properties. At the same time, compared with other cocatalysts (precious metals, metal oxides, metal sulfides), it has the advantages of low cost and high conductivity. Therefore, understanding the status of MQDs in the field of photocatalysis is crucial for their further development. In this review, we summarized the synthesis and modification methods of MQDs in recent years, as well as their photocatalytic applications in H_2 production, CO_2 reduction, N_2 fixation, pollutant degradation, and other aspects. In addition, the challenges and prospects faced by MQDs are also proposed, providing theoretical guidance for the further development of MQD–based photocatalysts.

1. Introduction

In the past few decades, the global industrialization process has accelerated, energy and environmental issues have become key factors restricting human survival and development [1–4]. Photocatalysis is one of the key methods to solve energy and environmental problems [5–7]. Since Fujishima and Honda first discovered in 1972 that TiO_2 electrodes can use sunlight to decompose water and produce H_2, photocatalysis technology has been widely studied [8]. Subsequently, the research on photocatalysts entered a rapid development stage, and various photocatalysts were reported, for example, $g-C_3N_4$, Bi_2O_3, MOFs, COFs [9–12]. However, due to low light utilization efficiency, fast charge recombination, and insufficient surface-active sites of photocatalysts, the catalytic activity of photocatalysts is far from meeting the requirements of practical applications. Therefore, researchers have constructed new photocatalysts through various methods to solve the above problems and improve photocatalytic activity [13–15].

In 2011, Naguib *et al.* [16] discovered a new type of two–dimensional material, MXenes, which are mainly obtained by selectively etching the "A" layer of the MAX phase (the chemical formula of MAX is $M_{n+1}AX_n$, where "M" represents an early transition metal, "A" represents an IIIA or IVA group element, "X" represents C and/or N elements, and $n=1, 2, 3$). Therefore, the chemical formula of MXenes is $M_{n+1}X_nT_x$ ("T_x" represents surface functional groups of the "M" layer, such as –O, –OH, –F) [17–19]. So far, more than 30 kinds of MXenes have been synthesized and more than 100 kinds of MXenes have been predicted [20]. MXenes have good hydrophilicity, high surface area, and excellent conductivity, with a surface redox capacitance of up to 2400 S/cm, equivalent to multilayer graphene [21], which has attracted increasing attention in many fields [22]. Compared with the two–dimensional form, quantum dot form (MQDs) can not only inherit the advantages of MXenes but also have better dispersibility, high stability, larger specific surface area, and easier functionalization due to the quantum confinement effect [23–25]. Based on this, in 2017, Xue *et al.* [26] broke down 2D MXenes into MQDs (Fig. 1A, lateral size

* Corresponding authors at: School of Environmental Science and Engineering, Zhejiang Gongshang University, Hangzhou 310018, China.
E-mail addresses: qiangli@zjgsu.edu.cn (Q. Li), wangqi8327@zjgsu.edu.cn (Q. Wang).

https://doi.org/10.1016/j.cclet.2023.109078
1001-8417/

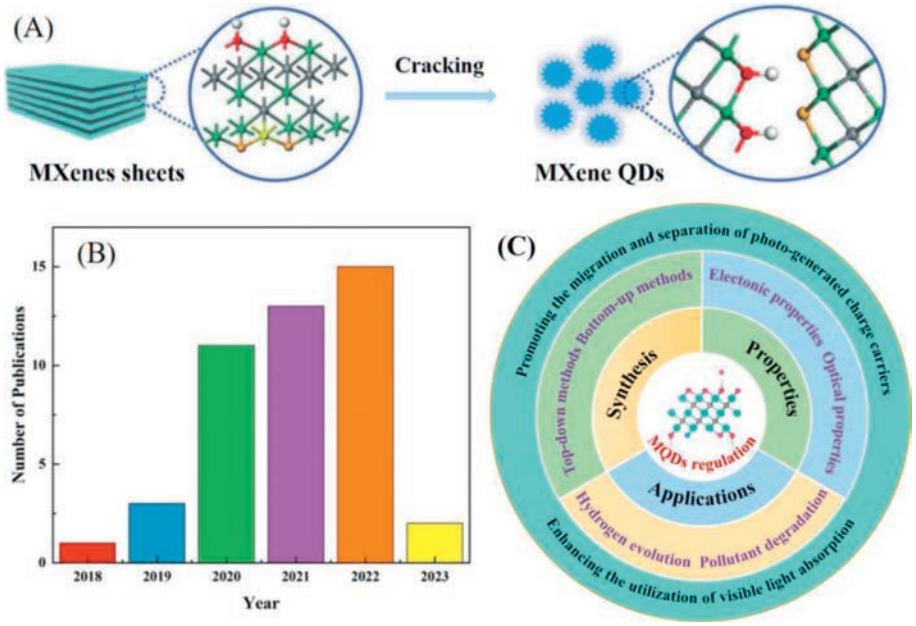

Fig. 1. (A) MQDs preparation diagram. Reproduced with permission [68]. Copyright 2022, Royal Society of Chemistry. (B) Number of MQDs published in journals. (Source: Web of Science, Keyword: MXene quantum dots and photocatalysis, Retrieval Date: December 30, 2022). (C) Overview of the synthesis, performance, and application of MQDs in the field of photocatalysis.

$\leq$ 10 nm) and applied them to cell imaging. The excellent and diverse characteristics of MQDs make them widely used in sensing, biomedical, optoelectronic devices, catalysis, and energy storage, among which they are particularly prominent in the field of photocatalysis [27–29]. Compared with other quantum dots, MQDs have better light absorption ability, which can absorb light in the range of ultraviolet to visible light, to achieve efficient catalytic reactions. The properties of MQDs can be adjusted by different preparation methods and surface modifications, so that they have better surface reaction performance and stability. Finally, MQDs have excellent electron transport properties, which can promote electron transport and shorten the time of electron recombination, and improve the photocatalytic efficiency. The above advantages make MQDs very suitable for photocatalytic application, and can effectively promote various photocatalytic reactions, such as water decomposition to produce H_2, photocatalytic reduction of CO_2 [30]. Therefore, MQDs have more application potential than MXenes (Fig. 1B). However, so far, research on the application of MQDs in photocatalysis is just beginning, and there is no comprehensive review on the application of MQDs in the field of photocatalysis. Therefore, this review summarizes the latest developments in MQD–based photocatalysts, focusing on the synthesis and modification methods of MQDs. The review also comprehensively introduces and analyzes the applications of MQD–based photocatalysts in recent years. Finally, the main challenges and development prospects of MQD–based photocatalysts are proposed (Fig. 1C). It is expected that this review can inspire for the development of MQD–based photocatalysts.

2. Synthesis and functionalization of MQDs

The synthesis and functionalization methods of MQDs have a crucial impact on their properties. By changing the synthesis and functionalization methods, the material size can be adjusted, the morphology and structure can be controlled to obtain the desired QDs structure and function [31–33]. So far, various methods have been used to synthesize different QDs, such as black phosphorus, Ti_3C_2, graphene [34–36]. MXenes have similar morphology and structure to other 2D bulk materials. Therefore, similar methods can be used to synthesize MQDs, mainly divided into top–down and bottom–up methods [37,38].

2.1. Top–down methods

The term "top-down approach" describes a technique for gradually downsizing big sizes to the nanoscale size using physical, chemical, or electrochemical processes [39,40]. This technique is perfect for large-scale production since it is simple to use, has an abundance of raw materials, yet produces poor products. For example, Cai group used HF to remove the Al layer from Ti_3AlC_2, and then intercalated with a tetramethylammonium hydroxide solution under sonication, and finally collected Ti_3C_2 QDs through twice centrifugations [41]. V_2C QDs could be prepared through a hydrothermal procedure in which ammonium hydroxide was used to reduce the size of V_2C [42]. The top-down approach can also be classified as hydrothermal technique, solvent thermal method, ultrasonic method, electrochemical method, and so on.

2.1.1. Hydrothermal method

Hydrothermal method is to simulate the growth process of crystals in the natural mineralization process, under a certain temperature and pressure, with water as the solvent, in a closed system to complete the reaction. The process mainly involves crystal nucleation and further growth. Under high temperature and pressure, 2D MXene sheets are cracked and assembled to form the desired MQDs. The size, morphology, and properties of MQDs can be adjusted by controlling the temperature, pH value, reactant concentration, and other conditions [43–45]. For example, Xu *et al.* [46] prepared Nb_2C QDs with good optical stability by hydrothermal method, whose average transverse size is 2.4 nm (Fig. 2A). Moreover, the average lateral sizes (ALS), average thickness (AT), and properties of Ti_3C_2 QDs could also be regulated by the hydrothermal reaction temperature [26]. Arising the hydrothermal reaction temperature causes Ti_3C_2 oxidation. The higher the temperature, the more TiO_2 is generated, which is accompanied with the change in structure. The prepared V_2C QDs showed good performance in photothermal therapy [47]. The TEM study confirmed that the higher hydrothermal reaction temperature was beneficial

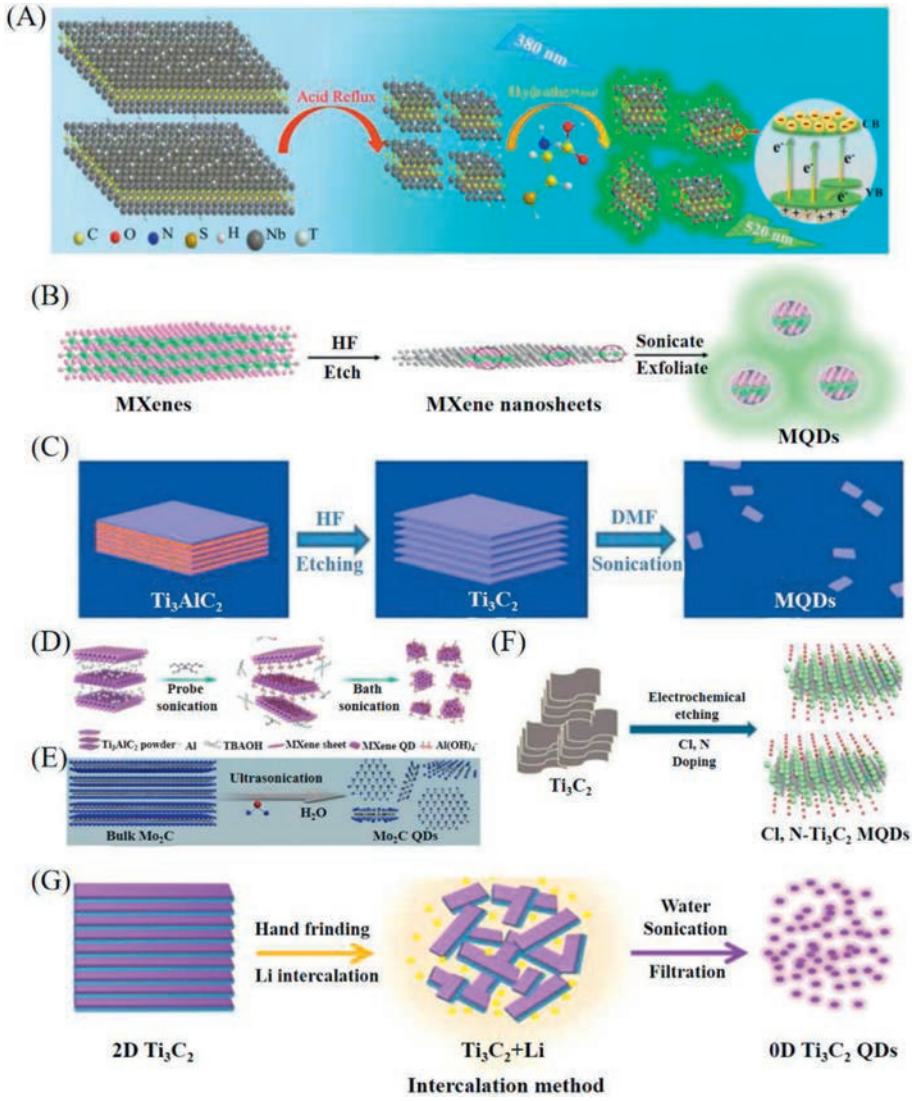

Fig. 2. (A) Schematic illustration of the hydrothermal synthesis of Nb_2C QDs. Reproduced with permission [46]. Copyright 2020, Royal Society of Chemistry. (B) Schematic diagram of the solvent thermal method for preparing MQDs. Reproduced with permission [50]. Copyright 2019, Royal Society of Chemistry. (C) Schematic diagram of the ultrasonic–solvent thermal method for preparing MQDs. Reproduced with permission [52]. Copyright 2021, Springer. (D) Schematic illustration of preparing MQDs by ultrasound method. Reproduced with permission [53]. Copyright 2017, Royal Society of Chemistry. (E) Schematic illustration of preparing MQDs by ultrasound–assisted liquid exfoliation method. Reproduced with permission [54]. Copyright 2018, Multidisciplinary Digital Publishing Institute. (F) Schematic illustration of preparing MQDs by electrochemical etching method. Reproduced with permission [58]. Copyright 2021, Elsevier. (G) Schematic illustration of preparing MQDs by intercalation method. Reproduced with permission [59]. Copyright 2022, Elsevier.

to the smaller size of MXene QDs (Figs. S1A–C in Supporting information) [48]. Therefore, the yield of QDs can be controlled by increasing the hydrothermal temperature. In general, the hydrothermal method is a simple and inexpensive method that can adjust the particle size and morphology of QDs by changing the reaction conditions.

2.1.2. Solvothermal method

The solvothermal method, using organic solvents as the reaction medium, was employed to fracture 2D MXenes into the desired MQDs. This method provides better control over the size and morphology of MQDs and is commonly utilized for MQD synthesis [49–51]. As shown in Fig. 2B, Zhang *et al.* [50] prepared Ti_3C_2 QDs with a size of 1.75 nm by stripping Ti_3C_2 in DMSO. Xu *et al.* [49] prepared different Ti_3C_2 QDs, named e–MQDs, f–MQDs, and s–MQDs, from Ti_3C_2 MXenes in ethanol, DMF, and DMSO solvents, respectively. The AT of all MQDs is between 1.0 and 2.5 nm, indicating a high degree of exfoliation and less layering. The size and quantum yield of MQDs are strongly influenced by the solvent's polarity, boiling temperature, and degree of oxidation. The boiling point of a solvent decreases as its polarity increases. Moreover, as the oxidative properties of the solvent decrease, the average lateral size of MQDs decreases, resulting in a higher quantum yield. In addition, the prepared dispersions display different photoluminescence (PL) colors under 365 nm excitation wavelength, with s–MQDs being white and e–MQDs and f–MQDs being blue. This indicates that the PL color of MQDs can be adjusted by changing the synthesis conditions, which is important for the study of MQDs' optical properties. Gao *et al.* [52] reported a ultrasonication–assisted solvothermal method to prepare Ti_3C_2 QDs. The average transverse size and thickness of Ti_3C_2 QDs were 2.75 nm and 1.02 nm, respectively (Fig. 2C). Ti_3C_2 MXene NSs can be more effectively fragmented into Ti_3C_2 QDs under ultrasonication. Compared with the hydrothermal method, the solvothermal method has no selection restrictions on the precursor materials, and it can be used to prepare QDs with different morphologies and

properties. The as–prepared QDs have high crystallinity, which is conducive to their performance improvement.

2.1.3. Ultrasound method

Different from hydrothermal/solvothermal methods, the ultrasound method utilizes shockwaves and cavitation induced by ultrasound to convert both layered and non–layered materials (MAX/MXenes) into MQDs. As shown in Fig. 2D, Yu *et al.* [53] first used a probe–type ultrasound to break down large Ti_3AlC_2 materials into smaller sizes, exposing more edges and surfaces. Then, OH^- reacted with exposed Al to form $Al(OH)_4^-$, weakening the interlayer binding force of Ti_3C_2 and forming Ti_3C_2 NSs. Finally, thinner MQDs were prepared using Ti_3C_2 NSs as precursors in a tetrabutylammonium hydroxide aqueous solution with an ultrasound bath under fluorine–free conditions. Dai *et al.* [54] reported the preparation of Mo_2C QDs with fewer layers by dispersing Mo_2C powder in ultra–pure water and subjecting it to ultrasound treatment (Fig. 2E). The MXenes (cavitated MAX) can be used to prepare MQDs by ultrasound method, instead of using hazards HF (or LiF/HCl). However, the low power density of ultrasound makes it difficult for large–scale production. In addition, this method has low utilization efficiency for synthesizing QDs and may produce side effects such as mechanical vibration and thermal effects.

2.1.4. Electrochemical etching method

Electrochemical etching is a simple and effective method for synthesizing QDs that have been used for various QD materials such as SiC QDs and ZnO QDs [55–57]. The advantage of this method is that it can avoid irreversible defects due to re–oxidation and prolonged exposure to ultrasonic radiation. Zhao *et al.* [58] used Ti_3AlC_2 and Pt as the working electrodes, tetramethylammonium hydroxide and NH_4Cl as the electrolyte to etch Al, which destroyed the Ti–Al bond and formed $AlCl_3$ (Fig. 2F). Due to the interaction between the defects or active edges of the carbon layer and the nearby atoms, the carbon layer was broken, and Cl^- reacted with Ti to form Ti–Cl. N in NH_4Cl is inserted into MQDs by forming new chemical bonds, resulting in Cl,N–MQDs. This method can control the size and morphology of MQDs by adjusting reaction conditions such as potential, current, and electrolyte composition. It can be performed at room temperature and pressure without requiring a high vacuum environment or high–temperature conditions, making it widely applicable. However, this method produces by–products or introduces other substances during MQD preparation, and the cost is relatively high, making it unsuitable for large–scale production of MQDs.

2.1.5. Other methods

In addition to the above–mentioned methods, several other approaches were also developed for synthesizing MQDs. For example, Jiang *et al.* [59] utilized Li^+ intercalation to cut 2D MXene NSs into 0D single–layer MQDs (Fig. 2G). Ti_3C_2 QDs, Nb_2C QDs, and V_2C QDs were prepared using this method. Zhang *et al.* [60] produced Ti_3C_2 QDs of different sizes by ball milling with various solid–state elements (C, S, P, Si). However, it is difficult to remove the solid–state elements from the final product, making it hard to synthesize composite materials. Moreover, Yuan *et al.* [61] focused laser beams on MXenes (dispersed in graphene) and induced plasma emission. By repeatedly burning particles with laser pulses, they reduced the particle size to make them more dispersed and uniform, ultimately resulting in transparent composite electrodes consisting of MQDs and reduced graphene oxide. Besides, Li *et al.* [62] injected liquid nitrogen into a $Ti_3C_2T_x$ layer, followed by heat input to remove water. Utilizing the temperature difference between liquid N_2 and heat can cause microexplosion to damage the structure of $Ti_3C_2T_x$, creating N–MQDs. The ALS and AT sizes were 7.23 nm and 5 nm, respectively.

Although top–down approaches have been widely used in MQDs synthesis, they inevitably suffer from low yield and poor reproducibility. Therefore, further research should be conducted to develop simple, cost–effective, high–yield, and reproducible methods to meet the demands of large–scale MQDs production in the future.

2.2. Bottom–up methods

The bottom–up method is another method of synthesizing nanomaterials, where small molecules or precursors are gradually assembled into nanostructures. Compared to the top–down approach, the bottom–up approach uses organic or inorganic precursors to achieve more precise control over the size, shape, and surface chemistry of QDs, and achieving higher precursor utilization and producing more structurally stable QDs [63–65]. The main methods for bottom–up preparation include molten salt synthesis and thermal decomposition.

Molten salt synthesis was a method that used salt as a solvent. Generally, the salts with low melting point were added to precursors, and by heating the mixture above the melting point of the salt, the melted salt can act as solvent. For example, Cheng *et al.* [63] homogeneously mixed molybdenum acetylacetonate precursor, sucrose, and NaCl. Mo_2C/C composite were obtained through a restricted space formed by NaCl nanocubes during heat treatment. The size of the Mo_2C QDs was 2–3 nm using HRTEM.

These studies provide insights into the bottom–up synthesis of MQDs. In order to meet the demand of mass production of MQDs in the future, it is necessary to further expand and improve the synthesis method to achieve the purpose of simple, mild, environmental protection and expanded production scale. Among them, the process of synthesizing MQDs by the precursor MAX is more critical: MXene material is obtained by etching the A layer of MAX materials. Then, MQDs is decomposed by hydrothermal, solvothermal, ultrasonic, electrochemical and other means to obtain MQDs (Table S1 in Supporting information). Optimizing these steps will help to improve the synthesis efficiency and quality of MQDs.

2.3. Functionalization of MQDs

Typically, MQDs have some inevitable drawbacks such as low production yield, tendency to aggregate, and susceptibility to oxidation [66]. These issues can be addressed through various energy–based methods, including surface modification, element doping, and coupling with other materials. During the synthesis of MQDs, surface groups such as –O, –F, and –OH can be generated, and the passivation of these surface groups is crucial for the performance and stability of MQDs [47]. Special functional groups can also be used to modify the surface of MQDs. For example, Lu *et al.* [67] modified Ti_3C_2 QDs with oleylamine as a surface passivating agent, improving their photoluminescence properties. Yuan *et al.* [68] used Sn^{2+} to modify the surface of Ti_3C_2 QDs, enhancing their light absorption and charge transfer capabilities. Besides, organic compounds can also be used to modify the surface of MQDs. Li *et al.* [69] used polyethyleneimine as a passivating agent to enhance the H_2 production ability of g–C_3N_4@Ti_3C_2 QDs. Zeng *et al.* [70] similarly used polyethyleneimine to modify Ti_3C_2 QDs, improving the CO_2 reduction ability of Ti_3C_2 QDs/Cu_2O nanowires/Cu. This indicates that surface modification of MQDs can improve their application performance in various fields, enabling them to play vital role in a wider range of applications. Element doping has many advantages and is commonly used for the energy–based fields. For example, Feng *et al.* [71] prepared N–doped Ti_3C_2 QDs using a solvothermal method. The doping of N reduced the particle size of MQDs and improved their fluorescence properties (Figs. 3A and B), resulting in a QY of 16.9%. Xu *et al.* [72] investigated S–doping,

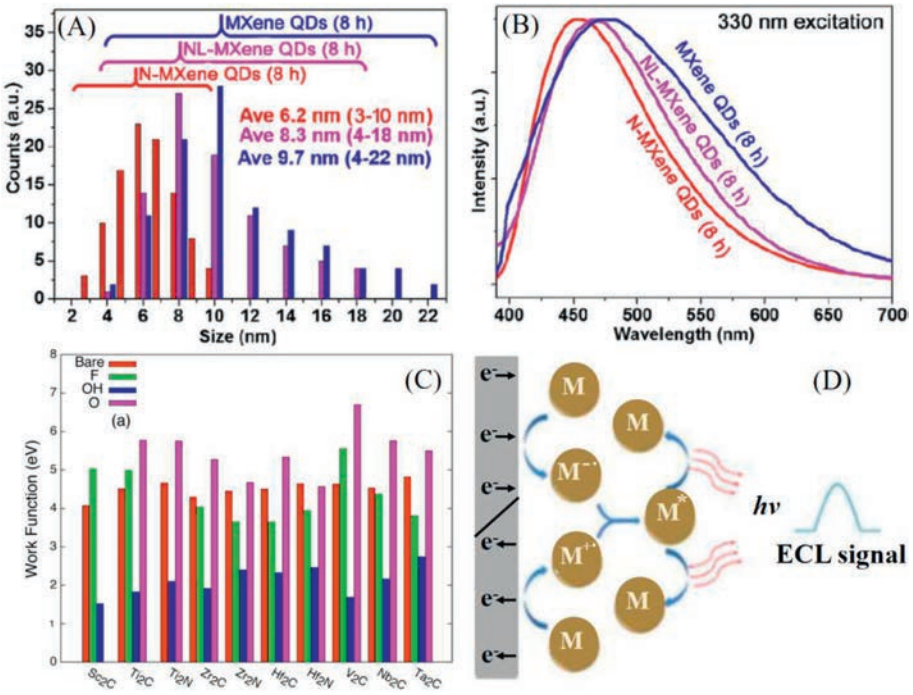

Fig. 3. (A) Particle size distribution of three types of MQDs, (B) PL emission spectra. Reproduced with permission [71]. Copyright 2020, Elsevier. (C) WF of different MXenes with different terminations. Reproduced with permission [79]. Copyright 2015, American Physical Society. (D) Schematic diagram of the quenching ECL pathway. Reproduced with permission [83]. Copyright 2018, Royal Society of Chemistry.

N–doping, and co–doping of Ti_3C_2 MQDs. Doped Ti_3C_2 QDs were connected to water molecules through hydrogen bonds, increasing the average lateral size of MQDs, a redshift in the emission spectrum, and a decrease in bandgap (E_g) with improved charge transfer ability. Zhao *et al.* [58] co–doped Cl and N elements into Ti_3C_2 QDs through electrochemical etching, resulting in Cl–N–Ti_3C_2 QDs with larger specific surface area and higher $^{\bullet}OH$ scavenging activity. Element doping can also enhance the photoelectric properties of MQDs by reducing their particle size, increasing photoluminescence lifetime (PLLT), and improving photoluminescence quantum yield (PLQY), laying the foundation for their application in the field of photocatalysis.

Forming composite materials with other materials is also a common method to improve their performance. Currently, various materials have been used to composite with MQDs. For example, Cheng *et al.* [63] reported the embedding of Mo_2C QDs into C NSs to form Mo_2C/C, which exhibited superior electrocatalytic N_2 reduction reaction performance. Isotope labeling experiments confirmed that the N element in the synthesized NH_3 originated from supplied N_2. Guo *et al.* [73] used Ti_3C_2 QDs to modify Ni and formed a flower–shaped hybrid material (Figs. S2A and B in Supporting information), significantly enhancing the catalytic reduction performance of Cr(VI). Although many studies on energy–based methods for MQDs have been conducted, they are still far from sufficient. In summary, current research on energy–based methods for MQDs mainly focuses on surface modification, element doping, and composite with other materials. These methods can improve the application performance of MQDs in different fields by changing their surface structure, functional groups, composition, and other aspects. However, there are still some challenges in the research of energy–based methods for MQDs. Firstly, the energy–based methods for MQDs are relatively complex and require considering the influence of multiple factors comprehensively. Secondly, the energy–based methods for MQDs also need to consider environmental stability and biosafety issues, requiring strict evaluation and verification. Therefore, further research on the mechanism and application of energy–based methods for MQDs is needed in the future, aiming to achieve more extensive applications in materials science, biomedicine, optoelectronics, and other fields.

3. The photoelectric characteristics of MQDs

Due to their unique composition and structure, 2D MXenes exhibit excellent electrical and optical properties that can be altered by changing the surface functional groups [74]. MQDs not only inherit these characteristics of MXenes but also show even better performance due to the quantum confinement effect [72]. Their outstanding properties increase the potential for applications of MQDs in various fields, particularly in the field of photocatalysis.

3.1. Electronic characteristic

The electrical transport properties of most MXenes are similar to metals, with the electrical resistivity decreasing as temperature increases. The electrical properties of MXenes are determined by their structure, composition, layer number, and surface functional groups [75]. MQDs not only inherit the advantages of MXenes, but also have higher specific surface area and quantum confinement effect [76]. Therefore, compared to MXenes, the electrical properties of MQDs should have more attractive surface functional groups, providing more possibilities for their practical applications. The unique composition of MXenes not only gives them metallic conductivity but also results in high electron density near the Fermi level (E_F), leading to excellent electrical conductivity. MXenes have a dual–metal layer structure both internally and externally, with the outer transition metal layer having a greater impact on their electrical conductivity [31]. Furthermore, MXenes exhibit high electrical conductivity and work function (WF), even higher than graphene (conductivity: 2000 S/m, WF: 4.42 eV) [77]. This indicates that MXenes can effectively promote charge transfer and can undergo surface plasmon resonance effects and form Schottky

barriers with semiconductors, thereby promoting photo–generated carrier separation. Recently, studies have shown that MQDs inheriting the advantages of MXenes can promote charge transfer more effectively. For instance, Xiao *et al.* [48] uniformly dispersed Ti_3C_2 QDs on the surface of nanosheets, forming a nano–dot/nano–sheet structure. Thus, the interfacial resistance and charge transfer were respectively reduced and promoted in Li–S batteries. Yu *et al.* [78] loaded Mo_2C QDs on N–doped graphene. These Mo_2C QDs have polarity and high conductivity, which can effectively inhibit shuttle effects in the material and improve its electrochemical and cycling performance.

In a word, MXenes mainly enhance the performance of photocatalytic materials by providing adsorption sites, promoting charge transfer, and accelerating photo–generated carrier separation. In addition, changes in the surface functional groups of MXenes can lead to the formation of new energy bands below E_F, resulting in a decrease in E_F and a change in the WF of MXenes. Electrons transfer from the transition metal to the electronegative surface terminal, causing the d–band to shift above E_F, significantly reducing the density of states and producing an energy gap (E_g) [31]. For example, Khazaei *et al.* [79] calculated the WF of MXenes using DFT and found that MXenes with –O as the surface functional group have a higher WF than those with –F and –OH (Fig. 3C). This is due to the reduction in E_F during surface energy–based modification of MXenes, resulting in an increase in WF for MXenes with –O and –F surface functional groups.

Kong *et al.* [80] studied the electronic structure of $Ti_3C_2O_2$ QDs loaded on monolayer graphene using DFT calculations and tested its H_2 evolution performance. The results showed that Ti_3C_2 QDs have a higher density of states near EF comparing to 2D MXenes NSs, and the –O end in Ti_3C_2 QDs can bring about strong local electric accumulation, which is more conducive to charge transfer. Zeng *et al.* [70] used DFT calculations to determine the electronic structure and E_F of Ti_3C_2 QDs with –O as the surface functional group and found that Ti_3C_2 QDs have rich electronic states near E_F, exhibiting excellent conductivity. These studies demonstrate that compared to MXenes, the more stable MQDs have superior electrical properties and can better promote photocatalytic reactions.

In conclusion, MQDs possess excellent photocatalytic properties due to their unique electronic structure and surface functional groups, providing more possibilities for their practical applications.

3.2. Optical characteristics

The optical properties of MQDs are crucial for their photocatalytic applications. The optical properties of MQDs mainly include light absorption, photoluminescence (PL), and electrochemiluminescence (ECL) [81], which can be adjusted through methods such as changing solvents, synthesis temperature, reaction time, pH, and so on [67].

Typically, the band structure of MQDs can be adjusted by changing their composition and surface functional groups, enabling significant light absorption from ultraviolet to near–infrared regions [82]. For example, Zeng *et al.* [70] loaded Ti_3C_2 QDs on Cu_2O nanowires to form a Ti_3C_2 QDs/Cu_2O NWs/Cu composite and analyzed their UV–visible diffuse reflectance spectra. The results show that loading Ti_3C_2 QDs on Cu_2O NWs/Cu can improve the optical absorption efficiency and broaden the optical absorption range. Different MQDs exhibit varying strengths of absorption in the near–infrared region, and can convert incident light energy into thermal, chemical, or other forms of energy, such as Ti_3C_2 QDs [53] and V_2C QDs [47] being used for cancer treatment or other applications. MQDs can exhibit strong PL emissions, but the corresponding reaction mechanism is not yet fully understood. Researchers usually study the fluorescence behavior of MQDs through PL color, fluorescence quantum yield, and fluorescence lifetime. Previous studies have reported that MQDs emit various colors of fluorescence (such as blue, green, red, and white) when excited at different wavelengths, with 365 nm being the most commonly used one. In addition, different MQDs can exhibit different colors under the same excitation wavelength due to their different compositions and preparation methods, and their PL colors can be controlled by changing the synthesis temperature, size, element doping, and other methods [83]. For example, Xue *et al.* [26] prepared Ti_3C_2 QDs using a hydrothermal method, and due to the influence of the core–shell structure, Ti_3C_2 QDs exhibited blue fluorescence at an excitation wavelength of 320 nm, and the emission spectrum of MQDs shifted from blue to red as the excitation wavelength increased within 340–440 nm, indicating that the bandwidth increased or energy level spacing decreased, making electron transitions easier. Feng *et al.* [71] prepared N–doped Ti_3C_2 QDs using a solvothermal method, and found that the charge transfer and separation ability of N–doped MQDs were much higher than those of undoped MQDs. Fig. S2C (Supporting information) shows the photoluminescence (PL) emission spectrum of N–MXene QDs at various excitation wavelengths. Increasing the excitation wavelength results in decreased PL intensity and a redshift in the emission spectrum of N–MQDs. This is because N doping can introduce more electronic energy levels, increase the probability of fluorescence emission, and thus improve the fluorescence lifetime. At the same time, it can also change the surface and edge states of MQDs, reduce the recombination of photo–generated carriers, and increase the fluorescence lifetime, indicating that N doping is an effective method to enhance the fluorescence performance of MQDs. Xu *et al.* [49] prepared three types of Ti_3C_2 QDs using DMSO, DMF, and ethanol as solvents, and found that MQDs exhibited a stronger quantum confinement effect in non–polar solvents, resulting in the maximum excitation and emission peaks shifting towards blue. Non–polar solvents do not interact with the surface groups of MQDs *via* hydrogen bond, reducing the screening effect of surface charges and increasing the surface energy of MQDs, thus altering their optical properties. This is of great significance for studying the properties and applications of MQDs in different environments.

In addition to light absorption and PL, the electrochemiluminescence (ECL) property of MQDs is also an important optical characteristic. ECL is a technique that utilizes electrochemical reactions to generate luminescence. In ECL systems, excited species are generated on the electrode surface through electrochemical reactions, and these species can transfer energy to the emitter *via* energy transfer or charge transfer, thereby stimulating its luminescence. ECL can effectively eliminate background signals, and its high sensitivity, wide detection range, and ease of scalability make it widely applicable in the fields of clinical diagnosis and food testing [84]. Qin *et al.* [83] first studied the ECL properties of Ti_3C_2 QDs in detail, by using annihilation processes and co–reactant enhancement (Fig. 3D). The ECL signal were detected and the generation pathway of ECL was proposed: MQDs receive electrons to form negatively charged $MQDs^{\bullet-}$, $MQDs^{\bullet-}$ oxidize and reduce MQDs to generate positively charged $MQDs^{\bullet+}$, and then electron transfer occurs between $MQDs^{\bullet-}$ and $MQDs^{\bullet+}$ to produce excited state of MQDs ($MQDs^*$), which emits light and transfers to the ground state of MQDs, generating the ECL signal. In addition, Xu *et al.* [49] investigated the ECL performance of three types of Ti_3C_2 QDs with different co–reactants, including $K_2S_2O_8$, L–cysteine, citric acid, H_2O_2, and glutathione. The results showed that the ECL signal of MQDs was significantly enhanced when using $K_2S_2O_8$ as the co–reactant, indicating that the presence of co–reactants can enhance the ECL signal. MQDs with higher light absorption coefficients and stronger electron donor properties can better transfer light energy, improving the efficiency of photocatalytic reactions. However, research on the optical properties of MQDs has mostly

focused on their PL properties, and further studies are needed to strengthen research on other optical properties such as light absorption, ECL, and photothermal conversion.

4. Photocatalytic applications of MQDs

In recent years, with the deepening research on MQDs, the application of MQD–based photocatalysts has gradually increased. Due to the interaction between the surface functional groups of MQDs and semiconductors, MQDs can be aggregated and adsorbed on the semiconductor surface. Moreover, its unique photoelectric properties not only enhance the visible light absorption of photocatalytic materials, but also receive photogenerated electrons from semiconductors, forming electron–hole pairs, improving the electron transfer rate, and promoting the progress of photocatalytic reactions. Therefore, MQDs have been applied in various fields, such as H_2 evolution, CO_2 reduction, N_2 fixation, and pollutant degradation [76].

4.1. H_2 evolution

H_2 is a well–known renewable energy source that can replace fossil fuels, thereby alleviating energy and environmental problems. Among them, the photocatalytic H_2 evolution reaction (HER) has received much attention since it can use solar energy to split water into H_2 [85]. Noble metals such as Au, Pd, and Pt are the most effective HER catalysts, which can promote the decomposition of water to H_2. However, due to the scarcity and expensive price of noble metals, their large–scale applications are limited. Therefore, seeking a low–cost and highly active material is of great significance. This alternative material should have HER catalytic activity similar to noble metals but at a lower price. Due to their unique photoelectric properties and high surface area, MQDs exhibit special catalytic activity for HER and are expected to become alternatives to noble metals [86]. MQDs are usually coupled with other semiconductors as electron acceptors or dielectrics to promote the separation of photo–generated carriers and enhance HER activity. For example, Yang *et al.* [87] prepared MQDs/ZIS/Ti(IV) by *in–situ* growth of Ti_3C_2 QDs on $ZnIn_2S_4$/Ti(IV) *via* electrostatic self–assembly. When Na_2S/Na_2SO_3 was used as a sacrificial agent, the H_2 production rate reached 7.52 mmol g^{-1} h^{-1}, which was 4.02 times higher than that of ZIS/Ti(IV) (Fig. 4A). This is mainly due to the interface charge transfer between MQDs and ZIS, which promotes HER. Dong *et al.* [88] reported that combining Ti_3C_2 QDs with TiO_2/g–C_3N_4 heterojunctions can effectively promote light absorption, charge separation and transfer, forming a more efficient HER catalyst. As shown in Fig. S3A (Supporting information), compared with TiO_2 and TiO_2/g–C_3N_4, the composite system has a smaller E_g and exhibits stronger HER performance [89], with H_2 evolution rates 98 times and 1.6 times higher than TiO_2 and TiO_2/g–C_3N_4, respectively (Fig. 4B). Yuan *et al.* [68] used highly conductive Sn^{2+}–modified Ti_3C_2 QDs (Sn–TQDs) as dielectrics, coupled with WO_3 and In_2S_3 to prepare WO_3/Sn–TQDs/In_2S_3, which was used for heavy metal reduction, organic degradation, and HER. As shown in the photocatalytic HER experiment (Fig. S3B in Supporting information), the H_2 evolution rate of WO_3/Sn–TQDs/In_2S_3 was significantly higher than WO_3 and In_2S_3, mainly because Sn–TQDs act as dielectrics, transferred electrons (e^-) from the conduction band (CB) of WO_3 to the valence band (VB) of In_2S_3 and combined with holes (h^+), resulting in the accumulation of a large number of e^- on In_2S_3, thus driving HER (Fig. S3C in Supporting information).

The above research shows that the introduction of MQDs can promote redox reactions and charge separation and transfer, significantly enhancing HER performance. However, research on the HER performance of MQDs is still insufficient, and the relevant mechanisms at the atomic layer level are not clear. Therefore, we need to invest more efforts to strengthen the research on MQDs.

4.2. CO_2 reduction

The removal and utilization of CO_2 have become a key issue for solving global warming. Currently, many methods have been used for CO_2 reduction, including photocatalysis, electrochemistry, photoelectrochemistry, and thermochemistry [90–93]. Among them, photocatalytic CO_2 reduction can convert CO_2 into hydrocarbons such as CO, CH_3OH, and CH_4 without consuming additional energy

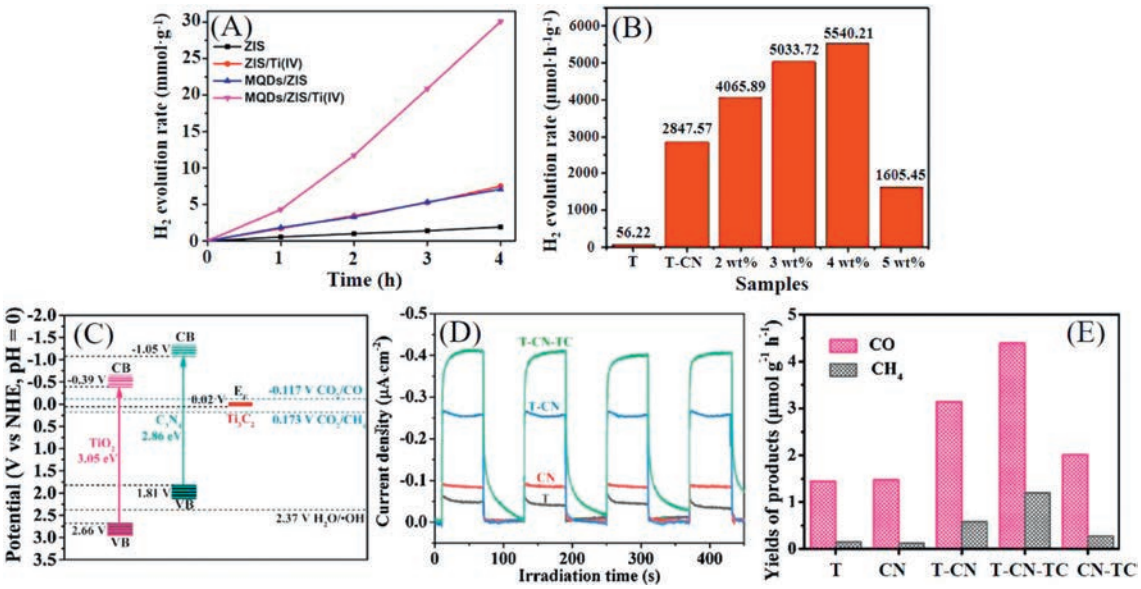

Fig. 4. (A) Comparative study of photocatalytic hydrogen production performance of different samples under simulated solar light irradiation. Reproduced with permission [87]. Copyright 2022, Multidisciplinary Digital Publishing Institute. (B) corresponding photocatalytic hydrogen evolution rate. Reproduced with permission [88]. Copyright 2021, American Chemical Society. (C) Energy band structure of TiO_2, C_3N_4 and T_3C_2 QDs, (D) Transient photocurrent response of T, CN, T–CN, and T–CN–TC, (E) The photocatalytic CO and CH_4 production rates of different samples. Reproduced with permission [95]. Copyright 2020, Elsevier.

sources, which not only solves global warming but also alleviates energy shortages and achieves renewable energy.

Currently, various photocatalysts have been used in CO_2 reduction research, but single–component photocatalysts usually have very low CO_2 reduction efficiency due to limited light absorption ability, poor adsorption, insufficient active sites, and rapid recombination of electron–hole pairs [94]. Therefore, researchers have developed multi–component photocatalysts by combining different photocatalysts to enhance the efficiency of CO_2 reduction.

In recent years, researchers have found that MXenes with high conductivity can be used as electron acceptors or dielectrics to promote the separation of photoinduced charge carriers and provide more active sites for CO_2 adsorption, significantly enhancing CO_2 reduction efficiency. MQDs inherit all the features of 2D MXenes and exhibit unique properties due to size confinement effects. However, because the preparation technology is not mature, single MQDs were not used as photocatalyst. Actually, MQDs are usually used as co–catalysts coupled with other semiconductors for photocatalytic CO_2 reduction. For example, Zeng *et al.* [70] coupled Ti_3C_2 QDs with Cu_2O NWs/Cu *via* electrostatic self–assembly to improve CO_2 reduction. The experimental results showed that after loading Ti_3C_2 QDs onto Cu_2O NWs/Cu, the light absorption range, cyclic stability, as well as separation of photoinduced charge carriers were all improved. As a result, the CH_3OH production rate by Ti_3C_2 QDs/Cu_2O NWs/Cu photocatalyst reached 153.38 ppm/cm^2 in 6 h, which was 8.25 times and 2.15 times higher than that by Cu_2O NWs/Cu and Ti_3C_2 NSs/Cu_2O NWs/Cu, respectively. Under sunlight illumination, Cu_2O is excited to produce e^- and h^+. However, because the CB energy level of Cu_2O is more negative than the E_F energy level of Ti_3C_2 QDs, Ti_3C_2 QDs act as electron acceptors, receiving e^- from Cu_2O and reducing CO_2 to CH_3OH.

Besides, He *et al.* [95] used Ti_3C_2 QDs to modify a core–shell structured TiO_2/C_3N_4, forming a 2D/2D/0D $TiO_2/C_3N_4/Ti_3C_2$ photocatalyst for CO_2 reduction. As shown in Fig. 4C, the E_F of C_3N_4 is higher than TiO_2 and Ti_3C_2 QDs. The photogenerated e^- is transferred from C_3N_4 to TiO_2 and Ti_3C_2 QDs, forming an intrinsic electric field that suppresses the recombination of photoinduced charge carriers. Therefore, the introduction of Ti_3C_2 QDs effectively promotes the separation of photoinduced charge carriers and enhances the photocatalytic performance of CO_2 (Fig. 4D), resulting in maximum CO and CH_4 yields that are 1.3 and 2 times higher than those of TiO_2/C_3N_4 photocatalysts, respectively (Fig. 4E).

Existing research is sufficient to demonstrate the important role of MQDs as co–catalysts in CO_2 reduction. However, current research is just beginning, and a more in–depth exploration is needed to understand the adsorption, activation, and charge transfer mechanisms, which will promote the development of MQDs in CO_2 reduction.

4.3. Nitrogen fixation

NH_3 is an important chemical raw material with wide applications in agriculture, aviation fuels and industrial production [96]. N_2 is considered the natural raw material for NH_3 production and the Haber–Bosch process is a common method in industrial production to fix N_2 into NH_3, but this reaction requires substantial fossil energy consumption and emits a lot of CO_2, which is not conducive to green chemistry [97]. Therefore, a low–energy–consumption and environmentally friendly N_2 fixation method is of great practical significance. Photocatalytic N_2 fixation has been widely studied due to its solar energy consumption and minimal environmental harm. Recently, research has shown that the unique properties of MQDs can be used to enhance photocatalytic N_2 fixation. For example, Qin *et al.* [98] synthesized Ti_3C_2 QDs/Ni–MOF for N_2 fixation by electrostatic self–assembly of Ti_3C_2 QDs and 2D nickel metal–organic frameworks (Ni–MOF). The Ni in the MOF material acts as an N_2 adsorption and activation site. Moreover, X–ray absorption near–edge structure test showed that the characteristic peaks A and B in Fig. 5A respectively originated from the π^* excitation of carbon ring structures and the transition of oxygen–containing groups/surface contaminants to sp^3 hybridized states. It can be seen from the figure that the characteristic peak A of 9MX–MOF is higher than that of Ni–MOF, while peak B is lower than that of Ni–MOF. This indicates that electrons may migrate from the carbon ring of Ti_3C_2 QDs to the external oxidized groups of Ni–MOF, causing a large accumulation of electrons on the CB of Ni–MOF, which helps to accelerate the conversion of N_2 to NH_3. Therefore, when Na_2SO_3 is used as a sacrificial agent, the photocatalytic N_2 fixation efficiency of Ti_3C_2 QDs/Ni–MOF can reach 88.79 μmol g^{-1} h^{-1}. In addition, Chang *et al.* [99] synthesized C_3N_4/r–Ti_3C_2 QDs by loading partially reduced Ti_3C_2 QDs (r–Ti_3C_2 QDs) on the surface of mesoporous hollow C_3N_4 spheres, which have abundant surface defects. The surface chemical properties of Ti_3C_2 were adjusted by using L–ascorbic acid and introducing oxygen vacancies (OVs) under the Ar atmosphere, followed by hydrothermal treatment to form r–Ti_3C_2 QDs with surface defects. The X–ray photoelectron spectroscopy (XPS) and electron paramagnetic resonance (EPR) of Ti_3C_2 MXenes and r–Ti_3C_2 QDs confirmed the existence of Ti^{3+} and OVs (Figs. 5B and C). MQDs promote the transfer and separation of photo–generated carriers, accelerating the conversion of N_2 to NH_3. Therefore, the NH_3 generation rates of C_3N_4/r–Ti_3C_2 QDs under white light and visible light were 1.6 and 1.9 times that of C_3N_4, respectively.

Overall, MQDs have great potential in the field of photocatalytic N_2 fixation, but related research is still in its early stages. Further exploration in this direction is necessary for achieving more efficient photocatalytic N_2 fixation.

4.4. Pollutant removal

In the past decades, photocatalysis has been widely applied in the removal of organic pollutants and toxic heavy metals [100,101]. Recently, MQD–based photocatalysts have also been developed due to their high conductivity, large specific surface area, and numerous surface functional groups. For example, Lai *et al.* [102] observed that Ti_3C_2 QDs can significantly enhance the photocatalytic performance of Bi_2O_3. The introduction of Ti_3C_2 QDs caused a red shift in the absorption edge of Bi_2O_3 and a decrease in E_g, thereby enhancing the light absorption of Bi_2O_3 and promoting the transfer and separation of photo–generated carriers. Consequently, after visible light irradiation for 90 min, the removal rate of tetracycline hydrochloride (TC) by Bi_2O_3/Ti_3C_2 QDs reached 82%, while the removal rate of TC by unmodified Bi_2O_3 was only 14%. In 2021, Yuan *et al.* [103] reported a new Z–type heterojunction WO_3/TQDs/In_2S_3, which employed Ti_3C_2 QDs as the dielectric layer between WO_3 and In_2S_3, and investigated its catalytic degradation activity towards Cr(VI) and bisphenol A (BPA). As shown in Figs. 5D and E, under visible light irradiation, WO_3/TQDs/In_2S_3 could reduce 99.8% of Cr(VI) within 12 min and degrade 97.6% of BPA within 120 min. Compared with WO_3/In_2S_3 without TQDs, WO_3/TQDs/In_2S_3 loaded with 3.9 wt% TQDs exhibited 4 times and 3 times higher degradation rates for Cr(VI) and BPA, respectively. The main mechanism is illustrated in Fig. S4A (Supporting information), where WO_3 and In_2S_3 are excited by light to generate e^- and h^+. Herein, TQDs act as a dielectric layer to transfer e^- from the CB of WO_3 to In_2S_3, thereby promoting the separation of photo–generated carriers and accelerating the photocatalytic degradation process. In 2022, Yuan *et al.* [45] replaced the dielectric layer between WO_3 and In_2S_3 using Sn^{2+}–modified Ti_3C_2 QDs (Sn–TQDs) with high conductivity. Compared with TQDs, Sn–TQDs not only enhanced the light absorption range of WO_3/Sn–TQDs/In_2S_3, but also further accelerated the transfer and separation rate of photo–generated

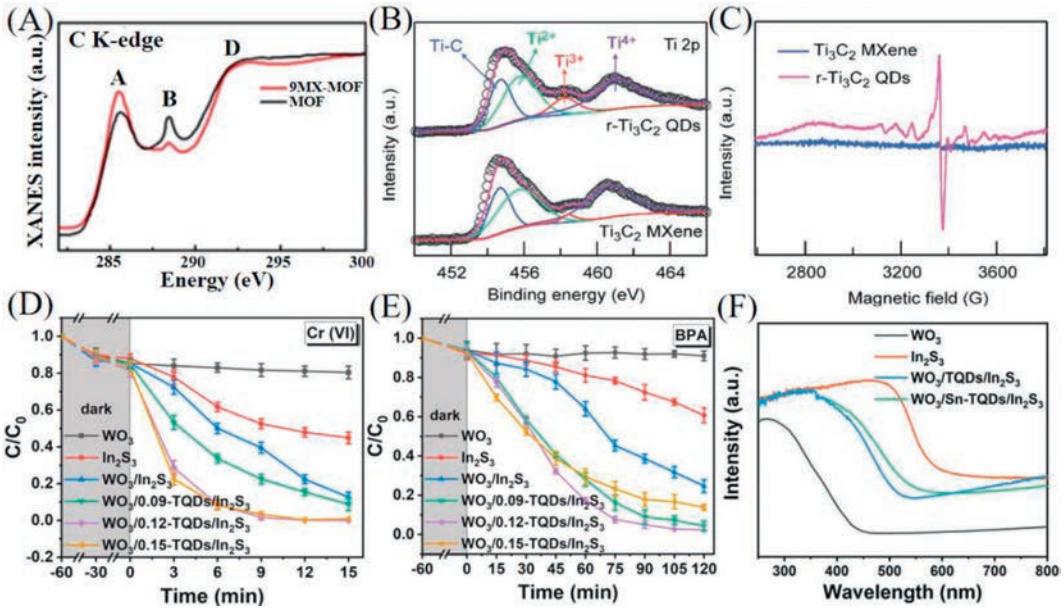

Fig. 5. (A) C K–edge XANES spectra of Ni–MOF and Ni–MOF with 9 mL Ti_3C_2 QDs added to the supernatant. Reproduced with permission [98]. Copyright 2020, American Chemical Society. (B) Ti 2p XPS spectra of Ti_3C_2 MXenes and r–Ti_3C_2 QDs, (C) EPR spectra. Reproduced with permission [99]. Copyright 2022, Royal Society of Chemistry. (D) Kinetics of photocatalytic reduction of Cr(VI) using different materials, (E) Kinetics of photocatalytic degradation of BPA. Reproduced with permission [103]. Copyright 2021, Elsevier. (F) UV–vis diffuse reflectance spectra. Reproduced with permission [68]. Copyright 2022, Elsevier.

carriers (Fig. 5F and Fig. S4B in Supporting information). Therefore, as shown in Fig. S4C (Supporting information), under visible light irradiation, WO_3/Sn−TQDs/In_2S_3 exhibited a 2.1 times higher rate towards Cr(VI) reduction than WO_3/TQDs/In_2S_3. In addition to organic pollutants and metal ions, MQDs are also used for NO removal. For example, Wang *et al.* [104] coupled SiC with Ti_3C_2 QDs to construct a novel heterojunction photocatalyst (Ti_3C_2 QDs/SiC). Under light conditions, Ti_3C_2 QDs/SiC can remove 74.6% of NO within 6 min, which is 3.1 times and 3.7 times higher than SiC and Ti_3C_2 QDs, respectively. This is mainly due to the strong interface contact between SiC and Ti_3C_2 QDs, which forms a heterojunction and accelerates the separation of photo generated charge carriers. In summary, MQD−based photocatalysts have significant advantages in organic pollutant degradation and heavy metal reduction, providing new pathways for photocatalytic applications.

4.5. Other applications

In addition, MQD−based photocatalysts have also been applied in other fields. For example, Lin *et al.* constructed Ti_3C_2 QDs−loaded defective g−C_3N_4 (TC/CN) *via* electrostatic self−assembly and applied it to produce H_2O_2. The highest H_2O_2 production rate by TC/CN reached 560.7 μmol/L, approximately 9.3 times that by bulk g−C_3N_4. The formation of numerous carbon vacancies in g−C_3N_4 leads to more delocalized electrons transferring to Ti_3C_2 QDs, causing the band edge to bend upward to form a Schottky barrier, thereby promoting the separation of photo−generated carriers [105]. In general, MQDs possess many surface-active sites, which can effectively adsorb and activate visible light. Additionally, MQDs exhibit excellent electron transport performance, which can promote the separation and transfer of photogenerated charges, thereby reducing their recombination rate and leading to enhanced performance.

Although there have been some studies on MQD−based photocatalysts in the field of photocatalysis, they are mainly focused on Ti_3C_2 QDs, and research on QDs with other metal centers is relatively scarce, which is not enough to fully demonstrate the important role of MQDs-based photocatalysis. Moreover, for other areas of photocatalysis, such as desulfurization and denitrification of fuels, sterilization, and organic synthesis, only MXene−based photocatalysts have been studied, and the application of MQDs in these fields has not yet appeared. Therefore, further exploration of MQDs in the field of photocatalytic applications is still needed.

5. Conclusions and outlook

This review provides a systematic and comprehensive summary of the current synthesis methods and modification strategies of MQDs. At the same time, the applications of MQDs in photocatalytic H_2 production, CO_2 reduction, N_2 fixation, and pollutant removal were mainly introduced. However, as a new type of photocatalytic material, MQDs still face several challenges and need to be improved.

5.1. Improvement of MQDs synthesis strategy

Typically, 2D MXenes are obtained from MAX *via* HF (or LiF/HCl) etching, followed by a top−down approach to prepare MQDs by cleaving the 2D MXene precursors. However, this method often presents significant safety risks as well as environmental pollution issues. The fluoride−free method can replace the etching of the "A" layer in MAX with HF (or LiF/HCl), which is not only safer and simpler but also enables the synthesized MQDs to exhibit superior performance. However, there is currently limited research on using fluoride−free methods to prepare MQDs and more exploration of such methods is urgently needed. Compared with the top−down approach, MQDs prepared by the bottom−up approach can provide better control over their size, morphology, and structural stability. In addition, different preparation conditions can be used to regulate the surface functional groups of MQDs, affecting the activity of MQD−based photocatalysts. Moreover, due to the small size of MQDs, traditional methods have difficulty in achieving uniform size during preparation with MXenes as precursors. Therefore, more efforts are needed in the synthesis of MQDs to achieve uniform size and stability.

5.2. Exploration of expanding non−Ti−based MQDs

So far, over 100 types of MXenes have been theoretically predicted, while over 30 types of MXenes have been experimentally synthesized in laboratories, providing a foundation for the diversified application of MQDs in the field of photocatalysis. The composition, layer spacing and functional group types of metal elements in MQDs have significant effects on their photoelectric properties, but currently, most research on MQDs in the field of photocatalysis is focused on exploring Ti_3C_2 QDs. Therefore, it is of great significance to expand the exploration of non−Ti−based MQDs to extend their light absorption range and improve the efficiency of photocatalytic reactions.

5.3. Expanding the application of MQDs photocatalysis

Expanding the application scope of MQD−based photocatalysts to solve practical problems is of great significance. Many studies have shown that the excellent physical and chemical properties of MQDs make them attractive in the field of photocatalysis. However, most current research on MQD−based photocatalysts is focused on H_2 production and pollutant degradation, with less research in other areas of photocatalytic applications such as H_2O_2 production, organic synthesis, antibacterial and antiviral applications. Moreover, most of the research has been focused on single or dual pollutant treatment systems. To this end, more attention should be paid to the treatment effects of multiple coexisting pollutants, to better apply MQD−based photocatalysts to the treatment of actual wastewater.

MQDs are a new type of nanomaterials, which have shown good application prospects in the field of photocatalysis. In the future, with the further research and development of MQDs, it will be possible to develop more efficient, flexible and environmentally friendly photocatalytic materials. In summary, there is still enormous potential to be explored for MQD−based photocatalysts. We should pay more attention to the above−mentioned issues, which are of great significance for promoting the rapid development of MQD−based photocatalysts. At the same time, we hope that this review can provide reference and inspiration for the research on MQD−based photocatalysts and promote their further development. With a deeper understanding of their mechanisms, we believe that more efficient and lower−cost MQD−based photocatalysts will be developed in the future.

Declaration of competing interest

The authors state that they have no known competing economic interests or personal relationships that could affect the work reported in this paper.

Acknowledgment

This work was supported by the National Natural Science Foundation of China (Nos. 22276168 and 21876154).

Supplementary materials

Supplementary material associated with this article can be found, in the online version, at doi:10.1016/j.cclet.2023.109078.

References

[1] D.J. Chen, Y.L. Cheng, N. Zhou, et al., J. Clean. Prod. 268 (2020) 121725.
[2] X.Y. Li, B.R. Jie, H.D. Lin, et al., J. Environ. Manag. 308 (2022) 114664.
[3] N. Olama, M. Dehghani, M. Malakootian, Appl. Water Sci. 8 (2018) 1–12.
[4] A. Touati, T. Hammedi, W. Najjar, et al., J. Ind. Eng. Chem. 35 (2016) 36–44.
[5] S. Zheng, H. Du, L. Yang, et al., J. Hazard. Mater. 447 (2023) 130849.
[6] B. Xue, Q. Li, L. Wang, et al., Chemosphere 332 (2023) 138829.
[7] Q. Wang, L. Wang, S. Zheng, et al., J. Hazard. Mater. 451 (2023) 131149.
[8] A. Fujishima, K. Honda, Nature 238 (1972) 37–38.
[9] Q. Guo, C.Y. Zhou, Z.B. Ma, et al., Adv. Mater. 31 (2019) 1901997.
[10] Q.H. Zhu, Z.H. Xu, B.C. Qiu, et al., Small 17 (2021) e2101070.
[11] Q. Wang, Q. Gao, A.M. Al-Enizi, et al., Inorg. Chem. Front. 7 (2020) 300–339.
[12] J. Guo, D. Ma, F. Sun, et al., Sci. China Chem. 65 (2022) 1704–1709.
[13] K.N. Van, H.T. Huu, V.N.N. Thi, et al., Chemosphere 289 (2022) 133120.
[14] A. Malathi, J. Madhavan, M. Ashokkumar, et al., Appl. Catal. A: Gen. 555 (2018) 47–74.
[15] Y. Fu, Y. Xu, Y. Mao, et al., Sep. Purif. Technol. 317 (2023) 123922.
[16] M. Naguib, M. Kurtoglu, V. Presser, et al., Adv. Mater. 23 (2011) 4248–4253.
[17] Y. Wei, P. Zhang, R.A. Soomro, et al., Adv. Mater. 33 (2021) e2103148.
[18] K. Rasool, M. Helal, A. Ali, et al., ACS Nano 10 (2016) 3674–3684.
[19] P. Kuang, J.X. Low, B. Cheng, et al., J. Mater. Sci. Technol. 56 (2020) 18–44.
[20] A. VahidMohammadi, J. Rosen, Y. Gogotsi, Science 372 (2021) eabf1581.
[21] A. Raza, U. Qumar, A.A. Rafi, et al., Sustain. Mater. Technol. 33 (2022) e00462.
[22] K.L. Huang, C.H. Li, H.Z. Li, et al., ACS Appl. Nano Mater. 3 (2020) 9581–9603.
[23] K. Zhang, D.Q. Li, H.Y. Cao, et al., Chem. Eng. J. 424 (2021) 130340.
[24] F.M. Yang, Y.Q. Ge, T. Yin, et al., ACS Appl. Nano Mater. 3 (2020) 11850–11860.
[25] G.H. Yang, J.L. Zhao, S.Z. Yi, et al., Sens. Actuator. B: Chem. 309 (2020) 127735.
[26] Q. Xue, H.J. Zhang, M.S. Zhu, et al., Adv. Mater. 29 (2017) 1604847.
[27] A. Rafieerad, W.A. Yan, A. Amiri, et al., Mater. Des. 196 (2020) 109091.
[28] X.Y. Jiang, H.J. Wang, Y. Shen, et al., Sens. Actuator. B: Chem. 350 (2022) 130891.
[29] F.F. Liu, S. Jin, Q.X. Xia, et al., J. Energy Chem. 62 (2021) 220–242.
[30] Y.H. Park, G. Murali, J.K.R. Modigunta, I. In, S.I. In, Front. Chem. 9 (2021) 734108.
[31] K. Hantanasirisakul, Y. Gogotsi, Adv. Mater. 30 (2018) e1804779.
[32] B. Bartolomei, J. Dosso, M. Prato, Trends Chem. 3 (2021) 943–953.
[33] W.F. Chen, G. Lv, W.M. Hu, et al., Nanotechnol. Rev. 7 (2018) 157–185.
[34] M.M. He, D. Wang, H. Shiigi, et al., Int. J. Hydrog. Energy 47 (2022) 17194–17203.
[35] J. Liu, Y.B. Shao, S.Y. Zuo, et al., Optoelectron. Adv. Mater. Rapid Commun. 16 (2022) 248–252.
[36] T.A. Tabish, H. Hayat, A. Abbas, et al., Curr. Opin. Electrochem. 30 (2021) 100786.
[37] Y.H. Xu, X.X. Wang, W.L. Zhang, et al., Chem. Soc. Rev. 47 (2018) 586–625.
[38] C.H. Zhao, X.B. Song, Y. Liu, et al., Nanobiotechnology 18 (2020) 1–32.
[39] T.J. Pillar-Little, N. Wanninayake, L. Nease, et al., Carbon 140 (2018) 616–623.
[40] H. Kang, D.Y. Kim, J. Cho, ACS Omega 8 (2023) 5885–5892.
[41] G.N. Cai, Z.Z. Yu, P. Tong, et al., Nanoscale 11 (2019) 15659–15667.
[42] D.P. Huang, Y. Xie, D.Z. Lu, et al., Adv. Mater. 31 (2019) 1901117.
[43] A. Rafieerad, W.A. Yan, G.L. Sequiera, et al., Adv. Healthc. Mater. 8 (2019) 1900569.
[44] D. Polsongkram, P. Chamninok, S. Pukird, et al., Phys. B: Condens. Matter 403 (2008) 3713–3717.
[45] M.M. ElFaham, A.M. Mostafa, E.A. Mwafy, J. Phys. Chem. Solids 154 (2021) 110089.
[46] Q. Xu, J.F. Ma, W. Khan, et al., Chem. Comm. 56 (2020) 6648–6651.
[47] Y. Cao, T.T. Wu, K. Zhang, et al., ACS Nano 13 (2019) 1499–1510.
[48] Z.B. Xiao, Z.L. Li, P.Y. Li, et al., ACS Nano 13 (2019) 3608–3617.
[49] G.F. Xu, Y.S. Niu, X.C. Yang, et al., Adv. Opt. Mater. 6 (2018) 1800951.
[50] Q.X. Zhang, Y. Sun, M.L. Liu, et al., Nanoscale 12 (2020) 1826–1832.
[51] M.A.A.B. Abdul Rani, N.A. Karim, N.S. Shamsul, et al., Fuel 345 (2023) 128271.
[52] X.H. Gao, X.C. Shao, L.L. Qin, et al., Nanoscale Res. Lett. 16 (2021) 1–8.
[53] X.H. Yu, X.K. Cai, H.D. Cui, et al., Nanoscale 9 (2017) 17859–17864.
[54] W.H. Dai, H.F. Dong, X.J. Zhang, Materials 11 (2018) 1776.
[55] J.Z. Chen, M.F. Chen, W.J. Zhou, et al., ACS Nano 16 (2022) 2461–2470.
[56] M. Mwania, C. Janaky, K. Rajeshwar, et al., Electrochem. Commun. 37 (2013) 1–4.
[57] L.C. Chen, N.N. Xu, H.Y. Yang, et al., Electrochim. Acta 56 (2011) 1387–1391.
[58] L. Zhao, Z. Wang, Y. Li, et al., J. Mater. Sci. Technol. 78 (2021) 30–37.
[59] B.W. Jiang, T. Yang, T.T. Wang, et al., Chem. Eng. J. 422 (2022) 136119.
[60] T.R. Zhang, X. Jiang, G.C. Li, et al., ChemNanoMat 4 (2018) 56–60.
[61] Y.J. Yuan, L. Jiang, X. Li, et al., Adv. Mater. 34 (2022) e2110013.
[62] X.S. Li, F. Liu, D.P. Huang, et al., Adv. Funct. Mater. 30 (2020) 2000308.
[63] H. Cheng, L.X. Ding, G.F. Chen, et al., Adv. Mater. 30 (2018) e1803694.
[64] K.A.S. Usman, J.W. Maina, S. Seyedin, et al., NPG Asia Mater. 12 (2020) 58.
[65] N. Abid, A.M. Khan, S. Shujait, et al., Adv. Colloid Interface Sci. 300 (2022) 102597.
[66] Q.W. Guan, J.F. Ma, W.J. Yang, et al., Nanoscale 11 (2019) 14123–14133.
[67] S.Y. Lu, L.Z. Sui, Y. Liu, et al., Adv. Sci. 6 (2019) 1801470.
[68] Z.T. Yuan, W.R. Tian, T.T. Ren, et al., Environ. Sci. Nano 9 (2022) 2417–2426.
[69] Y.J. Li, L. Ding, Y.C. Guo, et al., ACS Appl. Mater. Interfaces 11 (2019) 41440–41447.
[70] Z.P. Zeng, Y.B. Yan, J. Chen, et al., Adv. Funct. Mater. 29 (2019) 1806500.
[71] Y.F. Feng, F.R. Zhou, Q.H. Deng, et al., Ceram. Int. 46 (2020) 8320–8327.
[72] Q. Xu, W.J. Yang, Y.Y. Wen, et al., Appl. Mater. Today 16 (2019) 90–101.
[73] Y.L. Guo, Y.H. Cheng, X.C. Li, et al., J. Hazard. Mater. 423 (2022) 127053.
[74] D. Dhamodharan, V. Dhinakaran, H.S. Byun, Carbon 192 (2022) 366–383.
[75] M. Naguib, V.N. Mochalin, M.W. Barsoum, et al., Adv. Mater. 26 (2014) 992–1005.
[76] T.P. Nguyen, D.M.T. Nguyen, D.L. Tran, et al., Mol. Catal. 486 (2020) 110850.
[77] Z.Y. You, Y.L. Liao, X. Li, et al., Nanoscale 13 (2021) 9463–9504.
[78] B. Yu, D.J. Chen, Z.G. Wang, et al., Chem. Eng. J. 399 (2020) 125837.

[79] M. Khazaei, M. Arai, T. Sasaki, et al., Phys. Rev. B 92 (2015) 075411.
[80] Q.Q. Kong, X.G. An, L. Huang, et al., Front. Phys. 16 (2021) 53506.
[81] A.S. Sharbirin, S. Akhtar, J. Kim, Opto-Electron. Adv. 4 (2021) 200077.
[82] J.Y. Sui, X.F. Chen, Y. Li, et al., RSC. Adv. 11 (2021) 16065–16082.
[83] Y.L. Qin, Z.Q. Wang, N.Y. Liu, et al., Nanoscale 10 (2018) 14000–14004.
[84] S. Iravani, R.S. Varma, Nanomaterials 12 (2022) 1200.
[85] X. Du, T.Y. Zhao, Z.Y. Xiu, et al., Appl. Mater. Today 20 (2020) 100719.
[86] W.Y. Lei, T. Zhou, X. Pang, et al., J. Mater. Sci. Technol. 114 (2022) 143–164.
[87] L.Q. Yang, Z.H. Chen, X. Wang, et al., Nanomaterials 12 (2022) 542.
[88] G.M. Dong, Y.W. Zhang, Y.Y. Wang, et al., ACS Appl. Energy Mater. 4 (2021) 14342–14351.
[89] Z.Y. Wu, C.R. Li, Z. Li, et al., ACS Nano 15 (2021) 5696–5705.
[90] F. Fang, Y.X. Liu, X. Sun, et al., Appl. Surf. Sci. 564 (2021) 150407.
[91] N.Q. Zhang, X.X. Zhang, Y.K. Kang, et al., Angew. Chem. Int. Ed. 60 (2021) 13500–13505.
[92] S.Y. Yu, N.J. Yang, S.T. Liu, et al., Carbon 175 (2021) 440–453.
[93] X.D. Li, S.M. Wang, L. Li, et al., J. Am. Chem. Soc. 142 (2020) 9567–9581.
[94] S.C. Shit, I. Shown, R. Paul, et al., Nanoscale 12 (2020) 23301–23332.
[95] F. He, B.C. Zhu, B. Cheng, et al., Appl. Catal. B 272 (2020) 119006.
[96] X.Z. Chen, N. Li, Z.Z. Kong, et al., Mater. Horiz. 5 (2018) 9–27.
[97] L.X. Wang, Y. Xia, J.G. Yu, Chem 7 (2021) 1983–1985.
[98] J.Z. Qin, B.J. Liu, K.H. Lam, et al., ACS Sustain. Chem. Eng. 8 (2020) 17791–17799.
[99] B.B. Chang, Y.Z. Guo, H.L. Liu, et al., J. Mater. Chem. A 10 (2022) 3134–3145.
[100] Y.J. Fu, M. Tan, Z.L. Guo, et al., Chem. Eng. J. 452 (2023) 139417.
[101] H. Du, N.Y. Li, L.X. Yang, et al., Sep. Purif. Technol. 304 (2023) 122204.
[102] C. Lai, Z.W. An, H. Yi, et al., J. Colloid Interface Sci. 600 (2021) 161–173.
[103] Z.T. Yuan, H.S. Huang, N.J. Li, et al., J. Hazard. Mater. 409 (2021) 125027.
[104] H.M. Wang, R. Zhao, H.X. Hu, et al., ACS Appl. Mater. Interfaces 12 (2020) 40176–40185.
[105] S.F. Lin, N. Zhang, F.C. Wang, et al., ACS Sustain. Chem. Eng. 9 (2020) 481–488.